

Characterising the linkages of prevalent land use to anthropogenic heat flux and its impacts on the population in a coastal city of Kerala State, India

Pratheep Kumar B. *, Kerala and Emayavaramban V., Tamilnadu

Abstract

Quantitative observations on the potential effects of land use/land cover in fabricating urban microclimates are a precondition before every attempt of urban planning. The economy-driven brisk urban expansion initiatives invite severe environmental concerns worldwide. The burgeoning population pressure in the urban local bodies of the tropical cities led to jam-packed urban development's actuating surface urban heat island (SUHI) like anthropogenic heating phenomenon. In this paper, an attempt has been made to analyse the response of land surface temperature to changes in impervious and green cover densities from a spatial perspective and how it impacted the dwellers of the city of Thiruvananthapuram located in South India. The study revealed that Built-up is the single most significant contributor to the temperature rise of the area, with a land contribution index of 0.3. The SUHI exists at the city's core areas, covering the Central Business District (CBD) and the thickly populated zones with an average temperature of above 34.07°C in a zigzag manner. Even though the maximum temperature does not change spatially, the gap between maximum and minimum temperature decreases towards the densely populated zones of the city. It decreased the thermal comfort and increased vulnerability of health risks of people in the city region. The regression analysis suggests a marked spatial relation between land surface temperature, impervious cover, and green cover densities. The study provides valuable insights for mitigating SUHI by implementing sustainable blue-green infrastructures while providing comfortable, eco-friendly living to people.

Keywords: *Land use/land cover, land surface temperature, urban heat island, land contribution index, Thiruvananthapuram city.*

Introduction

By 2050, it is estimated that 68 percent of the world's population will reside in cities, with developing countries accounting for a substantial chunk of that total (United Nations, 2020). Rapid urbanisation transforms a predominantly rural agricultural land usage into a highly populated, dense built-up environment due to the migration

of the population into the urban settlements. In recent times, the capacity of our urban systems has been augmented in such a way as to accommodate more population. Unfortunately, many developing countries do not have adequate land use regulations to curb the harmful effects of such rapid growth. Rapid urbanisation in the cities of developing

nations is characterised by haphazard, unplanned building constructions and economic activity along the suburban areas which would change the underlying surfaces in specific places, altering the energy balance and introducing anthropogenic heating (Oke, 1982). Urban sprawl contributes to serious environmental problems like the urban heat island effect (UHI). The UHI phenomenon manifests in two types: atmospheric UHI (AUHI), measured by air temperature readings, and surface UHI (SUHI), measured by land surface temperatures (LST) (Fabrizi *et al.*, 2010). Owing to the accessibility of an extensive range of thermal remote sensing data at relatively high spatial and temporal resolutions (Voogt and Oke, 2003), SUHI methods are used to efficiently study the urban thermal environment (Kumari *et al.*, 2019). Several researchers have utilized the potential of various satellite sensors such as AVHRR of NOAA 7 satellite (Sobrino *et al.*, 2004), MODIS (Wan *et al.*, 2004), ASTER (Oguz, 2015), and the most popular and widely used Landsat TM and Landsat 8 OLI (Sobrino *et al.*, 2004; Weng *et al.*, 2004; Arulalaji *et al.*, 2010) for LST generation and analysis.

The morphological changes due to rapid urbanisation alter existing spatial patterns of LST. The changes include vegetation removal and its effect of low evaporation, high radiant temperatures due to increased insolation absorption and low albedo, blockage of wind passages, and decreased heat dissipation (Nuruzzaman, 2015). In tropical cities, it becomes disadvantageous, causing more energy consumption for cooling and refrigeration, increased pollution levels, and reduced thermal comfort to humans, particularly to vulnerable groups such as children and the aged. Incidence and

frequency of health risks such as respiratory, cardiovascular, and cerebrovascular illnesses are rising in urban areas as a result of UHI (Anderson and Bell, 201; Xu *et al.*, 2020, Markevych *et al.*, 2017). Besides, high temperatures affect the biodiversity of the urban space by upsetting the existing ecosystems (United Nations, 2020).

Urbanisation in India has shown a positive trend in the post-independence period due largely to economic growth, employment opportunities, migration from rural surroundings, improved transport and communication, and a better standard of living. However, they too face serious environmental problems of air and water pollution (Kaur, 2021), UHI development (Fabrizi *et al.* 2010), increased traffic congestion (Singh, 2012; Mohan, 2002), a lack of accessible housing, a decline in green spaces (Malik and Gupta; 2018) and issues with solid waste management (Kumar and Pandit, 2013).

Traditionally, Indian cities are characterized by their spatially unbalanced, highly polarized growth with sharp core-boundary distinction. On the other hand, the uniqueness of Kerala's urbanization is the development of an intense urban interaction zone with a co-existence of rural-urban functions alongside the major cities. Chattopadhyay (2021) observed that in Kerala, urbanization is spilling over from the main city and its satellite townships, and the intervening area becomes an intense zone of interaction and later urbanized. This spatial spread effect is more visible in all the three urban agglomerations of Kerala, namely, Kozhikkode, Kochi, and Thiruvananthapuram. The cities of Kerala are

also facing problems of urbanization similar to other cities of the country such as urban sprawl, loss of biodiversity, and changing urban microclimates.

The focus of the present study, Thiruvananthapuram city as the capital of the state is the administrative node for the whole state. As a fast-developing city in southern India, it is selected for the *smart city project* of the central government and improving its physical, social, and cultural infrastructure at a rapid pace. The city is surrounded by four satellite townships, namely Neyyattinkara, Kattakkada, Attingal, Kazhakkuttam and Kovalam with well-connected rail and road networks. The city is a favourite destination for migrants due to good transportation, the location of high-end educational and research institutions, IT hubs, and opportunities for government sector occupations.

The increased population concentration in the suburban regions mainly due to migration and rapid increase in the proportion of impervious surfaces in the city is responsible for problems that are similar to many other cities. Few studies have quantified the specific impacts of this rapidly changing urban microclimate on population and its various driving mechanisms such as land use, impervious surfaces, and blue-green spaces in the city. The present research fills this gap with the help of remote sensing and GIS techniques in order to help build a sustainable environment. To understand its spatial relation in the area, surface biophysical indices such as NDVI, NDBI, and LST have been correlated with each other. A population projection has been attempted and combined with LST to understand the environmental change in people.

Study area

The research area comes under the administrative boundary of Thiruvananthapuram, the southernmost district of Kerala. It comprises Thiruvananthapuram Corporation, adjoining 22 panchayats and two municipalities, spread over a total area of 694 km². The geographical boundaries of the study area are the Kottarakkara upland in the north, the Western Ghats in the east, the Vilappil uplands in the south, and the Arabian Sea coast in the west. The general elevation ranges from mean sea level to 1868mts (The Natural Resources Data Bank, 2013) towards the hilly stretches of the Western Ghats in an east-west direction. The area is drained by two perennial rivers and their tributaries originating from the Western Ghats, river Karamana in the north and Neyyar in the south. All these rivers empty into lagoon systems parallel to the coastal plain. The latitudinal and longitudinal extension of the study area is 8° 20' to 8° 40' north and 76°45'to 77° 5' east respectively. Figure 1 depicts the location of the study area.

The region lies in the monsoonal belt with alternate wet and dry conditions, favouring a geomorphic process dominated by weathering and erosion (Prasannakumar, 2007). Geomorphologically, the area is composed of ridges, isolated hills, river valleys, and a coastal plain. The coastal plain is characterized by sandy beaches, backwaters, and rocky promontories. Geologically the study area comprises of Khondalite group of rocks (Arulbalaji *et al.*, 2020).

As per Koeppen's climatic classification, the area falls under tropical monsoon, hot with seasonally excessive rainfall type. The mean annual temperature varies from 35°C in summer to 20°C in winter (Census, 2011). The

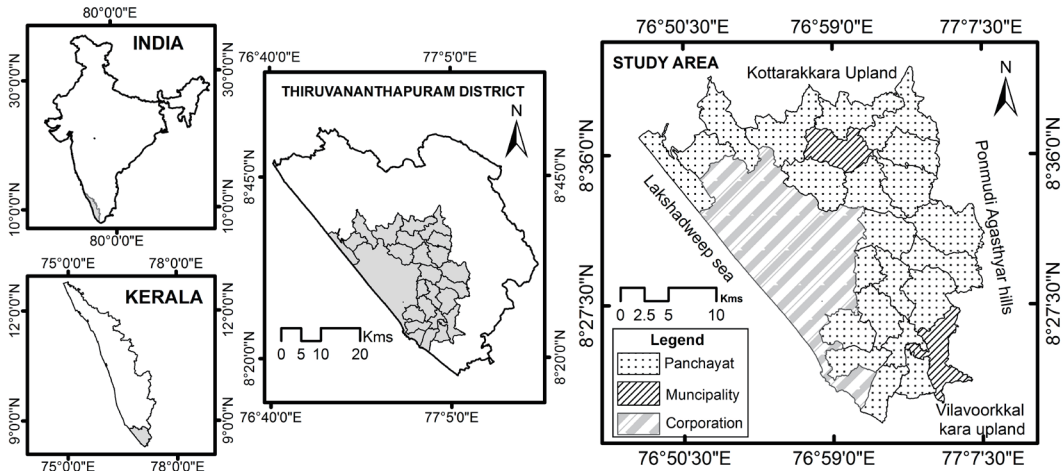


Fig. 1. Location of the study area

Table 1: Data sources

Satellite	Sensor	Acquired date	Path	Row	Bands	Resolution
Landsat 8	OLI	14/2/2021	144	55	Visible, NIR, and SWIR	30m
	TIRS-1	14/2/2021	144	55	Band 10	100m
	TIRS-2	14/2/2021	144	55	Band 11	100m
World view		10/12/2016				30m

southwest monsoon from June to September provides 68 percent of rainfall to the area with more than 250 cm annually. The climatic rhythm is characterized by four seasons, namely SW monsoon (June-September), a hot weather season (March-May), NE monsoon (October – November), and a winter season (December – February). Since the area is a coastal stretch, no well-pronounced winter and summer are experienced compared to interior locations (Census, 2011).

Data sources

For this research, the OLI/TIRS data set of Landsat 8 mission of the USGS, downloaded from [https://:earthexplorer.usgs.gov](https://earthexplorer.usgs.gov) website was used for generating land use/ land cover information, land surface temperature

patterns as well as the land cover indices. The boundary of the study area has been extracted from the nighttime city glow imagery of the world view earth data through the visual interpretation method. For convenience, the civic administrative boundaries covering the extracted area have been fixed as the study area boundary and have been collected from the Kerala State Land Use Board at a 1:375,000 scale. The details of the data sources are shown in Table 1.

Methods

Pre-processing of remote sensing data

Pre-processing, such as atmospheric and sun angle correction of the Landsat data is necessary for accurate results. The necessary correction has been done using the parameters

Table 3: Details of accuracy check performed

LULC types	User accuracy	Producer accuracy	Overall accuracy	Kappa statistic
Built up	90	90		
Mixed vegetation	91.6	91.6		
Paddy	100	85.7	91%	0.86
Plantation	83	100		
Sand	80	80		
Waterbody	100	100		

given in the metadata file using the raster calculator function of ArcMap 10.5.

Conversion of Digital Number (DN) to the top of the atmospheric reflectance (TOA) has been done using Eq.1

$$pA' = Mp * Qcal + Ap \dots \dots \dots \text{Eq.1}$$

Where pA' = Planetary Top of the atmosphere reflectance, Mp = Band specific multiplicative rescaling factor, Qcal = Quantized calibrated pixel value, and Ap = Band specific additive rescaling factor.

Sun angle correction of TOA is done using Eq.2

$$pA'' = pA' / \cos(\Phi) \dots \dots \dots \text{Eq. 2}$$

Where pA'' = sun angle corrected TOA, pA' = TOA and Φ = local sun elevation angle.

Land use land cover map generation

The LULC map of the Study Area has been generated from the corrected Landsat dataset by composing a False colour composite using Bands 3, 4, and 5 in ArcMap 10.5. The much-tested and widely used Maximum likelihood classification algorithm was employed for classifying the image as it is a measure considering the probability of a pixel falling in a particular class. An accuracy check of the generated LULC has been done using Google Earth imagery as a reference. Table 3 depicts the details of the accuracy check performed.

NDVI and NDBI computation

In remote sensing, the same parcel of land is portrayed in different spectral bands, providing the opportunity to generate thematic information by exercising multiple mathematical, logical, and Boolean operations. The normalized difference vegetation index is generated from the surface reflectance of Red and NIR bands using Eq. no. 3

$$NDVI = (NIR - Red) / (NIR + Red) \dots \dots \dots \text{Eq.3}$$

The NDVI output ranges from -1 to +1. -1 refers to the complete absence of vegetation, such as a waterbody, and +1 refers to dense vegetation. In the present study, the NDVI output has been classified to >0.35 after repeated trials of various thresholds to extract and identify vegetation.

Computing normalized difference built-up indices, built-up area information from satellite imageries can be obtained. The bare soils and built-up areas reflect more SWIR and NIR parts of the electromagnetic spectrum. The NDBI is computed by applying the following equation

$$NDBI = (SWIR - NIR) / (SWIR + NIR) \dots \dots \dots \text{Eq.4}$$

The NDBI value close to -1 indicates water bodies, and near to +1 shows thick

built-up. After manual calibration, the NDBI output is classified to above 0.3 to extract built-up.

Land surface temperature (LST) generation

The land surface temperature of the study area has been generated from the Band 10 of the TIR sensor. The TOA reflectance image (refer to eq.1) was input for computing the top of the atmosphere brightness temperature using the following equation.

$$T_b = k_2 / \ln(k_1(L\lambda + 1)) \dots \dots \dots \text{Eq.5}$$

Where T_b = Top of the atmosphere brightness temperature, k_1 and k_2 are the band-specific thermal conversion constants for Landsat 8, $L\lambda$ = wavelength of the emitted radiance and \ln = natural logarithm.

The conversion of T_b to LST was made through Equation No. 6

$$LST = (T_b - 273.15) / (1 + (\lambda * T_b - 273.15) / (\rho - 14380)) * \ln(\epsilon) \dots \dots \dots \text{Eq. 6}$$

Where $\rho = hc/\sigma$

h = planks constant ($6.626 * 10^{-34}$ J.S), c = velocity of light ($2.998 * 10^8$ m/s-1) and σ = Boltzmann constant ($1.38 * 10^{-23}$ J.k-1).

$$\epsilon = mP_v + n$$

$m = 0.004$ and $n = 0.986$ (value taken from Sobrino *et al.* (2004)

$$P_v = ((NDVI_{max} - NDVI_{min}) / (NDVI_{max} - NDVI_{min}))^2$$

Zonal statistical analysis

Concentric ring buffers, 300 metres apart, have been constructed around the central business district (CBD- the Thampanoor area), the city's commercial centre, to study the relationship between built-up and green

cover. To cover the entire study region, 82 zones have been constructed. The classified NDVI and NDBI outputs have been utilised to extract the zone-wise data using the zonal statistics tool in ArcMap 10.5. A fishnet with centre points (100×100 points) has been created, and the spatial analyst tool of ArcMap has been used to extract point source data from the outputs of LST, NDVI, and NDBI.

Computation of land contribution index

To understand the impact of underlying surface on land surface temperatures, the methodology of land contribution index (LCI), proposed by Huang *et al.* (2019) has been computed from the LULC and LST data sets. The LCI indicates the thermal contribution of an underlying surface to the temperature of the whole area. LCI is calculated using the following equation.

$$LCI = (T_i - T_m) P_i \dots \dots \dots \text{Eq. 7}$$

Where T_i = Mean temperature of the i th zone, T_m = Mean temperature of the whole area, and P_i = proportion of the i th underlying surface for the entire area.

An LCI value > 0 means the underlying surface positively contributed to the temperature hike of the area, and < 0 indicates a positive contribution to the temperature drop of the area.

LST transects and UHI delineation

Temperature profiles from the city centre to the rural-urban transition zones have been created to assess the mean temperature changes from the city centre to outward areas. Five transects were made from the CBD, approximately following primary cardinal directions and roads radiating from the city. Fig. 5 shows the transect profile. The urban

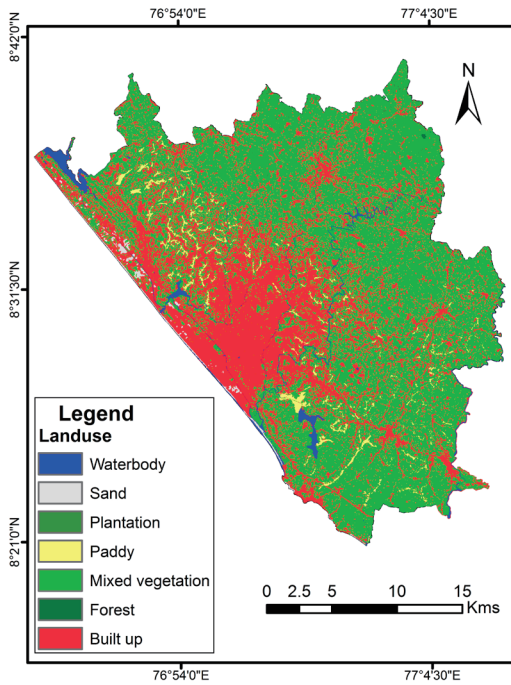


Fig. 2: Prevailing Land use land cover of the area

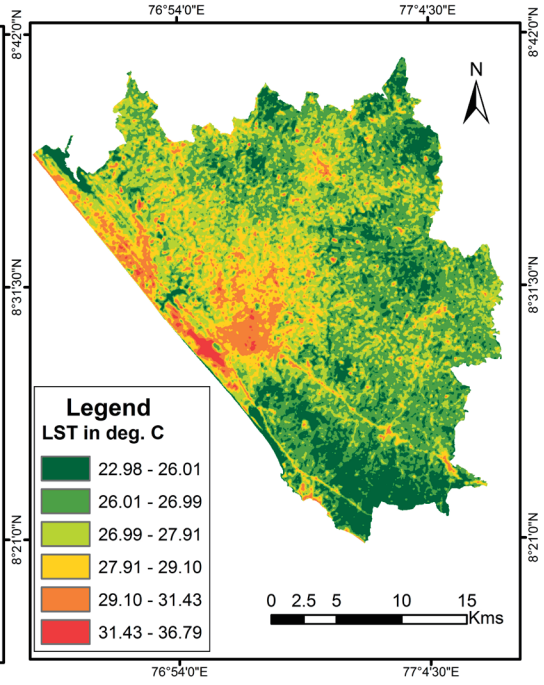


Fig. 3: Distribution of Land surface temperature

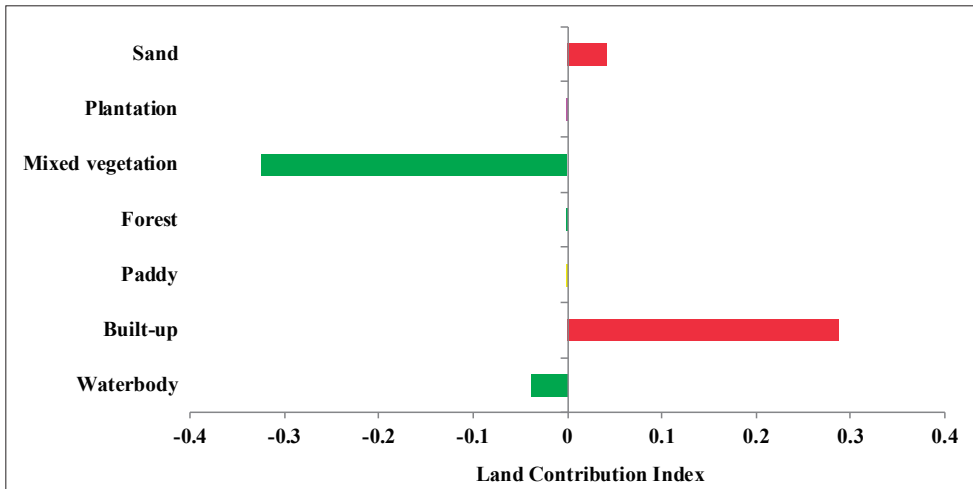


Fig. 4: LCI of various land use classes

Table 4: Landuse types and LST characteristics

Landuse	LST - Min	LST - Max	Range	Mean
Plantation	24.41	30.59	6.18	26.48
Built-up	23.75	36.79	13.03	28.09
Mixed vegetation	23.24	33.68	10.44	26.68
Waterbody	23.31	31.24	7.93	25.76
Forest	22.98	25.26	2.28	23.57
Sand	23.83	33.88	10.05	28.85
Paddy	24.28	29.76	5.47	26.74

heat island is delineated from the LST map using the following equation proposed by Ma *et al.* (2010)

$$LST > \mu + 0.5 * \delta \dots \dots \dots \text{Eq. 8}$$

Where μ is the mean and δ is the standard deviation of the LST of the urban area.

Trend line statistics

In order to assess the impact of LST on the population, linear trend line plots were created by inputting the maximum-minimum LST and population density of all the administrative units. Since the census data for 2021 is unavailable, a population projection has been made based on 2011 census data using the following exponential population equation.

$$Nt = Pe^{rt} \dots \dots \dots \text{Eq. 9}$$

Where, Nt = projected population, P = initial population (2011 census data), e = Logarithmic constant (2.71828), r = rate of increase of population divided by 100, and t = time interval.

Results and discussion

The spatial linkage between land use and LST

The various Land uses (Fig. 2) amounted to 694.71 km², about 31.99 percent of the total

area of the Thiruvananthapuram district. The dominant land cover of the area is mixed vegetation with 442.16 km² (63.64%). A significant proportion is covered by built-up (218.94 km²) followed by paddy fields 14.63 km² (2.14%), plantation agriculture 2.52 km² (0.36%), water bodies 12.03 km² (1.73%), and sandy beaches and sand-covered areas 4.43 km² (0.63%). A small stretch of land (0.017%) is covered by natural forest.

Many studies conclude that unplanned urbanization and haphazard suburban developments, including urban sprawl, have led to the development of urban heat islands in Thiruvananthapuram (Arulbalaji *et al.*, 2020; Ansar, 2010). The increased built-up density, reduced vegetation cover, and disrupted wind passages are factors that contribute to anthropogenic heating (Reis, 2008). Fig. 3 depicts the LST pattern in the study area, indicating a minimum temperature of 22.98°C and a maximum of 36.79°C with spatial variations based on land use types (Table 4).

Changes in temperature of different underlying surfaces

As is well-researched, the type of underlying surface greatly influences LST variation (Parvez *et al.*, 2021; Guo *et al.*, 2020). In

Thiruvananthapuram too, areas with built-up and sandy shorelines have significantly higher LST due to their ability to heat up rapidly and emit intense radiation. In contrast, areas covered by vegetation and water bodies have a cooling effect. Thiruvananthapuram is characterized by a mix of plantation agriculture and mixed vegetation in the northern, northeastern, and eastern sides and low-lying paddy fields and water bodies, such as the VellayaniKayal, in the southern and southeastern sides.

Combining LCI and temperature classes, results show that the performance of each underlying surface in the whole area differs considerably, indicating the role of the underlying surface in surface heating. It is also observed that the LCI of green spaces is more than that of water bodies in contributing to the cooling of the area (Fig. 4), and the findings are congruent with the earlier observations of Tarawally *et al.* (2018) and Wang *et al.* (2019). Both the green spaces and water bodies contribute positively to the area's cooling. However, fewer such spaces in the 3 km radius of the CBD virtually turn the area into an urban heat island.

Spatial patterns of LST and UHI

The city of Thiruvananthapuram is well-connected to the surrounding satellite townships and other district headquarters of the state by an intricate network of rail and road systems. The city's spatial expansion is seen along the main arterial roads, resulting in a linear strip corridor type of urban form. In this section, we have analysed the temperature variations between the city centre and its rural outskirts with the help of transects following major roads and cardinal directions (Fig. 5 & 6). The results reveal that

the LST averages within a 3 km radius of the city centre touch the critical limit of 34.07°C set for the delineation of the urban heat island (UHI) (see Eq. 8). The study employs the UHI delineation methodology as proposed by Ma *et al.* (2010) which is deemed most suitable for cities with a coastal location such as Thiruvananthapuram (Shafahad *et al.*, 2021). Although the city's UHI average is lower than other tropical cities, Thiruvananthapuram's maritime location coupled with high relative humidity can exacerbate surface heat for city dwellers. The North, Northeast, and Southeastern profiles display greater variability as they traverse through urban corridors that connect to satellite townships like Kazhakkuttam, Nedumangad, and Neyyattinkara.

LST variation with changing NDVI and NDBI

According to our analysis of land use indices, the normalized difference vegetation index (NDVI) values exceeding 0.3 are observed in the North, Northeastern, and eastern rolling plains as well as isolated hilly areas, where plantation agriculture and mixed vegetation are the predominant land use types. Moreover, the southeastern and southern parts adjacent to the backwaters have higher vegetation cover. Our findings reveal that the impervious surface cover and average land surface temperature (LST) gradually decrease towards the rural-urban fringe and beyond. Regression analysis suggests that the explanatory power of the variable average land surface temperature (LST), in determining its relationship with green cover density ($R^2=0.733$) is weaker compared to its relationship with impervious cover densities ($R^2=0.781$). A significant positive correlation

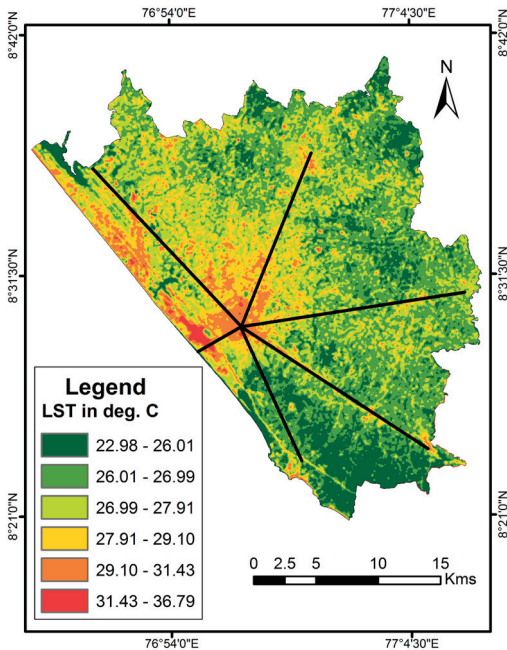


Fig. 5: Temperature transects along the LST map

is observed between average LST and impervious cover density ($r = 0.884$), while it is negative over average LST and green cover densities ($r = -0.856$). This is primarily because of the differences in thermal conductivity and heating capacity of underlying surfaces (see Fig. 7). Built-up surfaces and rigid pavements absorb insolation rapidly and retain heat for a longer duration whereas vegetation cover provides shading to the land surface and releases energy through the

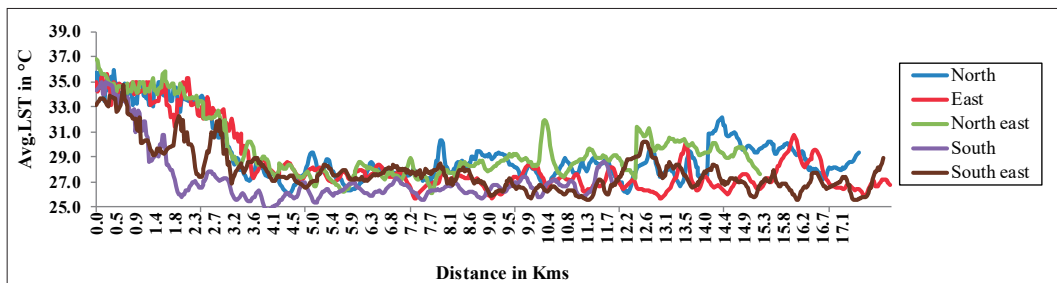


Fig. 6: Temperature profiles of the major transects from the city centre

evapotranspiration process (Marzban et. al., 2018; Shahfahad et al., 2020).

Our analysis further reveals that the spatial distribution of green cover is heterogeneous in the area, and this could aggravate the UHI phenomenon in the city. Additionally, the NDVI and LST relationship is expected to change seasonally and over time, as the deciduous vegetation, mostly rubber plantations in the hills shed their canopies during the dry summer season. Figure 9 illustrates the extent of urban development within the region, highlighting the highest intensity observed within the central urban zones characterized by a normalized difference built-up index (NDBI) value of 0.411. Conversely, Figure 10 depicts the spatial distribution of vegetation coverage across the area, as indicated by a normalized difference vegetation index (NDVI) value approaching 0.60, indicating the presence of dense vegetation cover in the fringe zones of the city.

Within the UHI zone of Thiruvananthapuram city, the percentage of impervious cover is observed to be more than 80 percent, comprising predominantly of residential, commercial, institutional, industrial built-up, and transport pavements. The green cover, comprising urban parks and

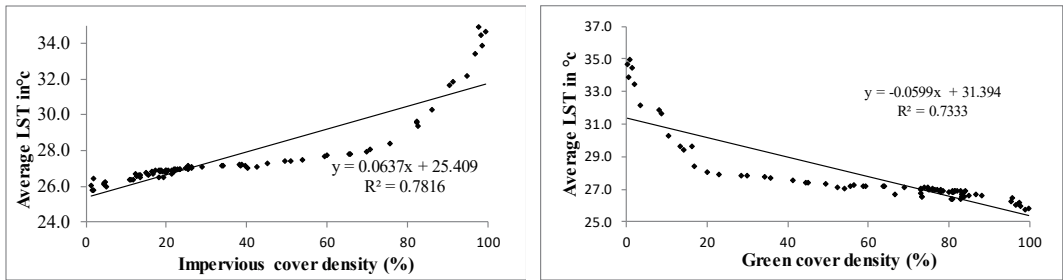


Fig. 7: Correlation plots between average LST and impervious cover density (A) and green cover density (B)

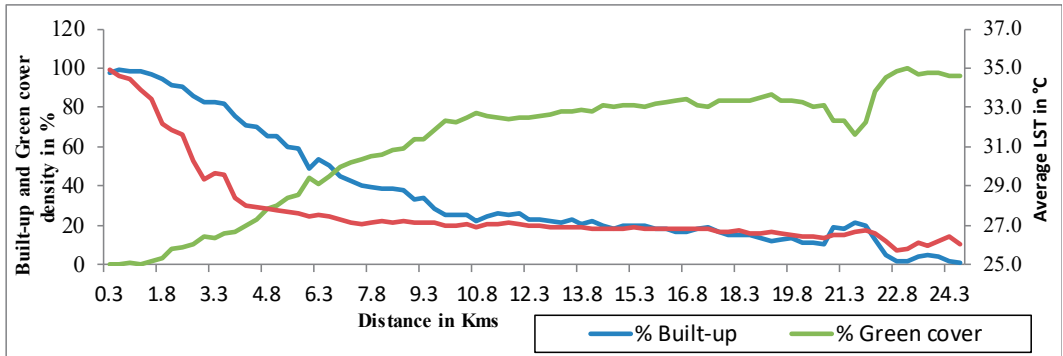


Fig. 8: Spatial relation of LST and Built-up, green cover densities and the UHI zone

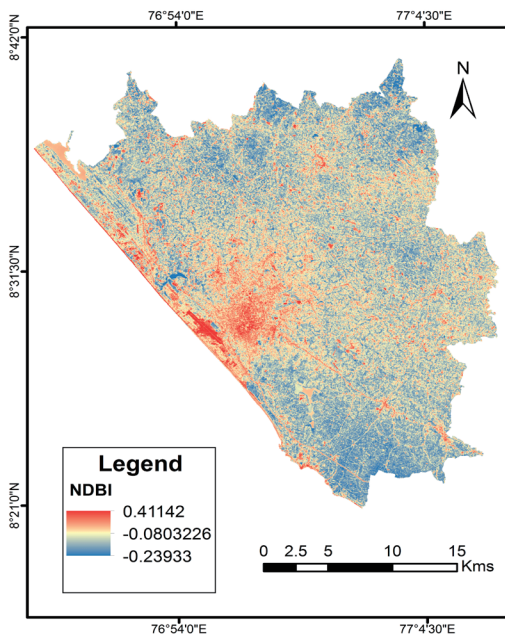


Fig. 9: Normalized difference Built-up index

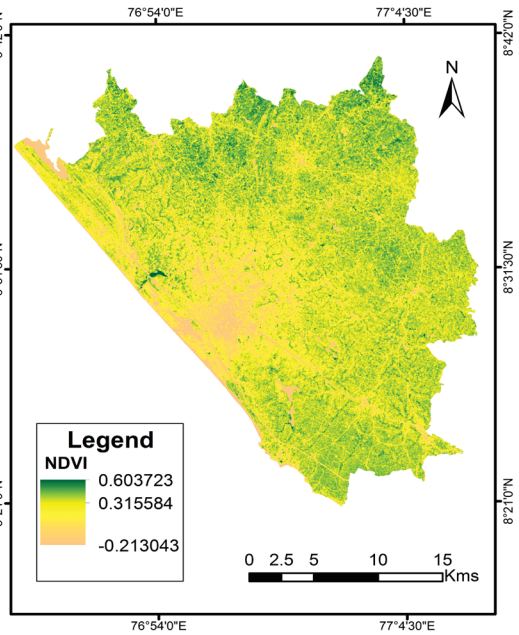


Fig. 10: Normalized difference vegetation index

institutional greenery, is sparsely distributed and accounts for less than 20 percent of the total area. This limited green cover is insufficient to counterbalance the high level of radiational heat generated by the concrete structures during the day. However, at distances ranging from 6 to 20 km from the city, the built-up density diminishes and green cover is sufficient to reduce the temperature to an average of 27°C. At a distance of 20 to 23 km, satellite townships are rapidly developing and are interconnected by an outer ring road that promotes suburban development in an arc-like pattern. Figure 8 demonstrates a sharp decline in green cover and a simultaneous increase in impervious cover and LST in this region. The finding underscores the need to prioritize green infrastructure in urban planning and development policies to mitigate UHI effects.

Effect of LST on the population

The spatial distribution of the population within the study area exhibits non-uniform patterns, characterized by concentrated densities in the central and coastal regions, while the Panchayats located on the eastern and northern fringes display lower population densities. Notably, a significant portion of the population is concentrated in five specific corporation wards, where population densities exceed 20,000 persons per km². Moreover, within the city's core, there are 24 wards with high population densities above 10,000 persons per km². These densely populated areas experience an average LST of 30.1°C or higher and are frequently affected by the UHI effect.

Moving away from the central core, 41 corporation wards display medium population densities exceeding 5,000 persons per km²,

experiencing an average surface temperature of 28.1°C. Furthermore, nine Panchayats bordering the corporation, two satellite town Municipalities, and 27 corporation wards exhibit low population densities ranging between 2,500 and 5,000 persons per km² where the average temperature is recorded at 27.3°C. Notably, thirteen Panchayats and two corporation wards have very low population densities, below 2,500 per km². These regions enjoy substantial vegetation cover, leading to an average LST reduction of 26.3°C.

With population and economic activities growing, there is a greater demand for residential expansion. The temperature of the residential areas is increasing inevitably because most of the concrete residential buildings are equipped with additional metallic roofing to reduce indoor temperatures. However, these metallic roofs have higher thermal conductivity and significantly increase the surrounding temperature. Previous studies by Cui *et al.* (2016) and Zhou *et al.* (2004) have shown that urbanization has a significant effect on climate, leading to the development of UHI.

Figure 11 shows that the maximum temperature is rarely affected by population density ($R^2 = 0.001$), while the difference in the diurnal range of temperature decreases with increasing population density ($R^2=0.444$). As a result, the increasing trend of minimum temperatures towards the city disturbs the thermal comfort of the people and makes them vulnerable to living, requiring more energy for cooling, refrigeration, and maintaining indoor temperatures. It also has severe health effects on potentially vulnerable populations such as children under 10 years and the elderly above 60 years by disturbing

their sleeping patterns.

Several studies have explored the relationship between disturbed sleeping patterns and vulnerability to Coronary Artery Diseases. For example, Sadabadi *et al.* (2023) in their study of Mashhad city in Iran found that the incidence of coronary heart disease is significantly higher in people with shortened night sleep duration. Similarly, Krishnan *et al.* (2016) also found a higher risk of coronary artery diseases (CAD) among urban men and women compared to their rural counterparts in the Thiruvananthapuram district. Other contributory risk factors to CAD such as obesity, diabetes, and high blood pressure, are also high in the urban area (Joseph, 2000). Additionally, a survey conducted by the government medical college hospital of over 50,000 people for two consecutive years in Thiruvananthapuram city has revealed an alarming prevalence of irregular heart rhythm disease (0.9%) and heart failure rates (1.69%) that are among the highest reported rates in the country (Maya. C, 2022). Dhorde (2009) noted a trend of increasing annual maximum temperatures in Thiruvananthapuram with a rate of change measured at 0.30°C per decade. Furthermore, there is a noticeable rise in minimum temperatures across the West Coast, contributing to a significant escalation in thermal discomfort and heat stress within the city. This trend, as highlighted by Desai (2017), appears to have predominantly emerged post-1990s.

The above discussion substantiates that the changing microclimate of the city would be a cause for increasing the residents' health risks that negatively impact the quality of life. Needless to say, further research is needed to firmly establish the relationship between

rising temperature and increasing health risks in the area.

Conclusion

This study examines the interplay between land use, land surface temperature (LST), and the spatial distribution of population, green cover, and built-up densities in Thiruvananthapuram city and its surroundings. Investigations revealed that the level of urbanization is relatively high in the study area with a significant proportion of built-up areas consisting of residential colonies, corporate establishments, and government institutions and offices due to the city's status as the state's administrative capital. The thick, compact developments in the city's core areas lead to higher LST (Fig. 12). Although urbanization and changes in population densities do not appear to affect the area's maximum temperature, the gap between LST minimum and maximum decreases toward densely populated areas, leading to the development of the urban heat island phenomenon (Fig. 13).

The study identifies that the UHI is spread over a 3 km radius area, covering the central business district and densely populated areas in a zigzag manner, extending further towards the airport and urban corridors connecting the city with satellite hubs. Regression analysis shows that LST has a stronger relationship with impervious cover than with green cover densities, indicating the ability of concrete and other rigid built-ups to intensify the UHI effect. The absence of available vacant land within the city proper indicates a need to explore alternative approaches, such as rooftop gardening, green walls, vertical

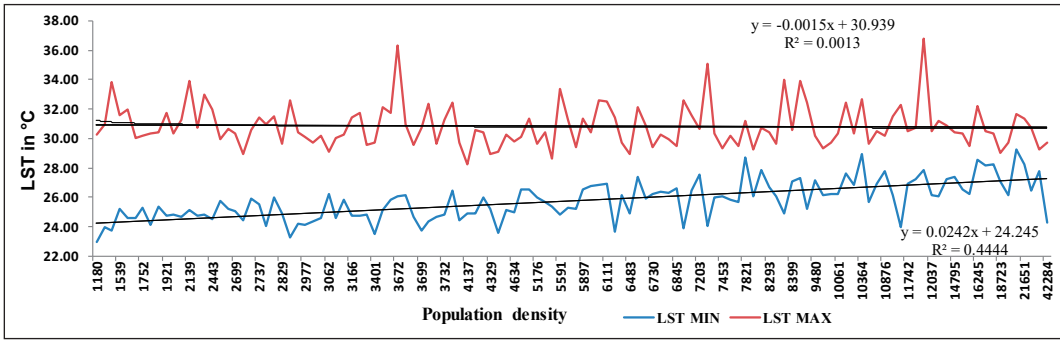


Fig. 11: Population density of the administrative units in relation to maximum – minimum LST

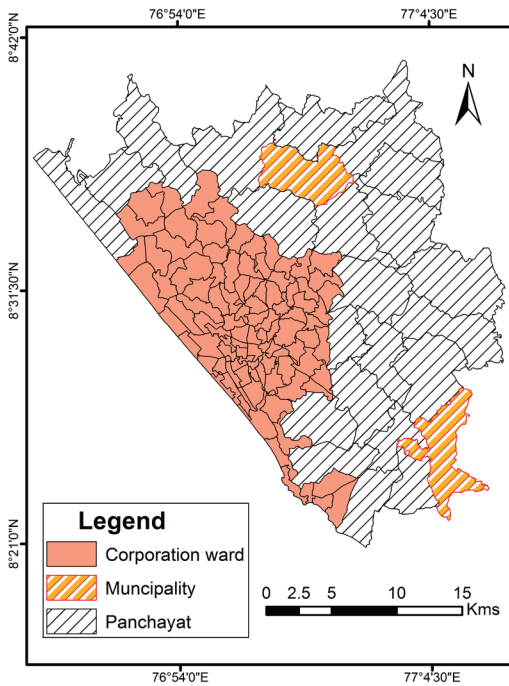


Fig. 12: Local bodies of the study area

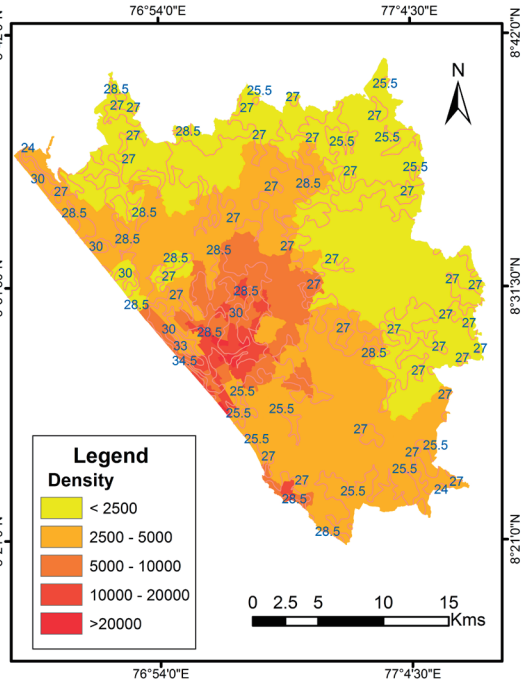


Fig. 13: Projected population density, 2021

gardening, and cool roofing techniques, to mitigate the urban heat island (UHI) effect. At a distance of 8 km from the city centre, a significantly high vegetation cover gives rise to the reduced average temperature of 27.3°C. This finding presents an opportunity for planners and urban designers to formulate plans and policies to protect the vegetation

cover from complete removal.

References.

Anderson, G. B., & Bell, M. L. (2011). Heat waves in the United States: Mortality Risk during Heat waves and effect modification by Heat wave characteristics in 43 US communities. *Environmental Health perspectives*. Volume 119(2), pp 210 – 218. <https://doi.org/10.1289/>

- ehp.1002313.
- Ansar, S., Dhanya, C. R., Thomas, G., Chandran, A., John, L., Prasanthi, S., Vishnu, R., & Zachariah, E. J. (2010). A study of Urban/Rural cooling rates in Thiruvananthapuram, Kerala. *Journal of Indian Geophysical Union*, Volume.16(1), pp 29-36.
- Arulbalaji, P., Padmalal, D., & Maya, K. (2020). Impact of Urbanization and Land surface temperature changes in a coastal town in Kerala, India. *Environmental Earth Science*, Volume 79(400). <https://doi.org/10.1007/s12665-020-09120-1>.
- Chattopadhyay, S. (2021). *Geography of Kerala*. Concept Publishing Company Pvt. Ltd., New Delhi- 110059. ISBN 93-5439-001-3.
- Cui, Y., Xu, X., Dong, J., & Qin, Y. (2016). Influence of urbanization factors on surface urban heat island intensity: A comparison of countries at different developmental phases. *Sustainability*, Volume 8 (706)
- Desai, M. S., & Dhorde, A. G. (2018). Trends in thermal discomfort indices over western coastal cities of India. *Theoretical and Applied Climatology*, Volume 131, pp 1305–1321. <https://doi.org/10.1007/s00704-017-2042-8>
- Dhorde, A., Wakhare, A. (2009). Evidence of long-term climate change at Major cities of India during the Twentieth century. *The International Journal of Climate Change: Impacts and Responses*, Volume 1(3), ISSN:1835 – 7156.
- Fabrizi, R., Bonafoni, S., & Biondi, R. (2010). Satellite and ground based sensors for the Urban Heat Island analysis in the city of Rome. *Remote sensing*, Volume 2, pp 1400 – 1415.
- Guo, A., Yang, J., Sun, W., Xiao, X., Xia, C. J., & Jin, C. (2020). Impact of Urban Morphology and Landscape characteristics on spatiotemporal Heterogeneity of Land surface temperature. *Sustainable cities and Society*. Volume 63 (102443). <https://doi.org/10.1016/j.scs.2020.102443>.
- <https://doi.org/10.1186/s12872-016-0189-3>.
- Huang, Q., Huang, J., Yang, X., Fang, C., & Liang, Y. (2019). Quantifying the seasonal contribution of coupling Urban Landuse types on Urban Heat island using Land contribution Index: a case study in Wuhan, China. *Sustainable cities and society*. Volume 44, pp 666-675. <https://doi.org/10.1016/j.scs.2018.10.016>.
- Joseph, A., Raman. K. & Soman, C. R. (2000). High risk for coronary heart disease in Thiruvananthapuram City: A study of serum lipids and other risk factors. *Indian heart journal*. Volume 52, pp 29-35.
- Kaur, R., & Pandey, P. (2021). Air Pollution, Climate Change, and Human Health in Indian Cities: A Brief Review. *Frontiers in Sustainable Cities*. Volume 3, pp 1- 18.<https://doi.org/10.3389/frsc.2021.705131>.
- Krishnan, M. N., Zachariah, G., Venugopal, K., Mohanan, P. P., Harikrishnan, S., Sanjay, G., Jeyaseelan, L., & Thankappan, K. R. (2016). Prevalence of coronary artery disease and its risk factors in Kerala, South India: a community-based cross-sectional study. *BMC cardiovascular disorders*, Volume 16, Issue12.
- Kumar, V., & Pandit, V. K. (2013). Problems of solid waste management in Indian cities. *International Journal of Scientific and Research publications*, Volume 3, Issue 3. ISSN 2250-3153.
- Kumari, M., Sharma, K., & Sharma, R. (2019). Using Moran's – I and GIS to study the spatial pattern of Land Surface Temperature in relation to Landuse/ Landcover around a thermal powerplant in Singrauli district, Madhya Pradesh, India. *Remote Sensing Applications: Society and Environment*, Volume15 (100239). <https://doi.org/10.1016/j.scs.2020.102443>.

- org/10.1016/j.rsase.2019.100239.
- Ma, Y., Kuang, Y., & Huang, N. (2010). Coupling urbanization analysis for studying urban thermal environment and its interplay with biophysical parameters based on TM/ETM+ imagery. *International Journal of Applied Earth Observation and Geoinformation*. Volume 12(2), pp 110 – 118.
- Malik, K. T., & Gupta, A. (2018). Open Green Spaces in Urban Indian Cities, Its Importance, Rapid Decline and Restoration Strategies. *International journal of scientific research and review*, Volume 07, Issue 4. ISBN 2279-543x
- Markevych, I., Schoierer, J., Hartig, T., Chudnovsky, A., Hystad, F., & Dzhambov, A. A. (2017). Exploring pathways Linking Green space to Health: Theoretical and Methodological Guidance. *Environmental Research*, Volume 158, pp 301 – 317. <https://doi.org/10.1016/j.envres.2017.06.028>.
- Marzban, F., Sodoudi, S., & Preusker, R. (2018). The influence of land-cover type on the relationship between NDVI–LST and LST-Tair, *International Journal of Remote Sensing*, Volume 39:5, pp 1377-1398. <https://doi.org/10.1080/01431161.2017.1402386>.
- Maya, C. (2022). Study finds high prevalence of A-fib, heart failure in Thiruvananthapuram. *The Hindu daily*, May 30, 2022. <https://www.thehindu.com/news/cities/thiruvananthapuram-study-find-high-prevalance-of-A-fib-heart-failure-in-Thiruvananthapuram-The-Hindu>.
- Mohan, D. (2002). Traffic Safety and Health in Indian cities. *Journal of Transport and Infrastructure*. Volume 9(1). Pp 79-94. <https://www.researchgate.net/publication/23535732>.
- Nuruzzaman, M. (2015). Urban heat islands causes, effects and mitigation measures- a review. *International Journal of Environmental Monitoring and Analysis*, Volume 3 (2), pp 67 – 73.
- Oguz, H. (2015). A software tool for retrieving Land surface temperature from ASTR imagery. *Journal of agricultural sciences*, Volume 21(4), pp 471 – 482.
- Oke, T. R. (1982). The Energetic basis of the urban heat island. *Quarterly Journal of Royal Meteorological Society*. Volume 108(455), pp 1 – 24.
- Parvez, I. M., Aina, Y. A., & Balogun, A. L. (2021). The influence of Urban form on the spatio-temporal variations in Land surface Temperature in an arid coastal city. *Geocarto International*, Volume 36 (6), pp 640 – 659. <https://doi.org/10.1080/10106049.2019.1622598>.
- Prasannakumar, V. (2007). *Geomorphology of Kerala*. International Centre for Kerala Studies, University of Kerala, Kariavattom. ISBN 81-87590-15-7.
- Reis, S. (2008). Analysing landuse/ landcover changes using remote sensing and GIS in Reize, North-East Turkey. *Sensors*, Volume 8, pp 6188-6202. <https://doi.org/10.3390/s8106188>.
- Sadabadi, F., Darroudi, S., Esmaily, H., Asadi, Z., Ferns, A. G., Mohammadpour, H. A., Noorian, H. A., Ghayour-Mobarhan, M., & Moohebat, M. (2023). The importance of sleep patterns in the incidence of coronary heart disease: a 6-year prospective study in Mashhad, Iran. *Scientific Reports*, Volume 13(2903). <https://doi.org/10.1038/s41598-023-29451-w>
- Shahfahad, R. M., Naikoo, M. W., Ali, M. A., Usmani, T. M., & Rahman, A. (2021). Urban Heat Island Dynamics in Response to Land-Use/Land-Cover Change in the Coastal City of Mumbai. *Journal of the Indian Society of Remote Sensing*, Volume 49, pp 2227 - 2247. <https://doi.org/10.1007/s12524-021-01394-7>.

- Singh, S. (2012). Urban transport in India: Issues, challenges, and the way forward. *European Transport – Trasporti Europei. Issue 52, Paper -5, pp 1 – 26, ISBN 1825-3997*. <https://www.researchgate.net/publication/286966258>
- Sobrino, J. A., Jimenez-Munoz, J. C., & Paolini, L. (2004). Land surface temperature retrieval from LADSAT TM 5. *Remote sensing of Environment*, Volume 90, pp 434 – 440.
- Tarawally, M., Xu, W., Hou, W., & Mushore, T. (2018). Comparative analysis of responses of Land surface temperature to Long term Land use / cover changes between a coastal and inland city: A case of Freetown and Bo town in Sierra Leone. *Remote sensing*, Volume 10(1), Issue 112. <https://doi.org/10.3390/rs10010112>.
- United Nations. (2019). *World population prospects : Highlights*, United Nations Department for Economic and Social Affairs. Newyork.
- United Nations. (2020). *The 17 Goals*. <https://sdgs.un.org/goals>.
- Voogt, J. A. & Oke, T. R. (2003). Thermal remote sensing of urban climates. *Remote Sensing of Environment*, Volume 86, pp 370 – 384.
- Wan. Z., Zhang. Y., Zhang. Q & Li. Z. L. (2004). Quality assessment and validation of the MODIS global land surface temperature, *International Journal of Remote Sensing*, Volume 25(1), pp 261-274. <https://doi.org/10.1080/0143116031000116417>
- Wang, Y., Zhan, Q. & Ouyang, W. (2019). How to quantify the relationship between spatial distribution of Urban waterbodies and Land Surface Temperature? *Science of Total Environment*. Volume, 671, pp 1 – 9. <https://doi.org/10.1016/j.scitotenv.2019.03.377>.
- Weng, Q., Lub, D. & Schubringa, L. (2004). Estimation of land surface temperature-vegetation abundance relationship for Urban Heat Island studies. *Remote sensing of environment*, Volume 89, pp 467- 483.
- Xu, G., Chen, L., Chen, Y., Wang, T., Shen, F. H., & Wang, K. (2020). Impact of Heat waves and cold Spells on the Morbidity of Respiratory diseases: A case study in LanZhou, China. *Physics and Chemistry of the Earth*, parts A/B/C, Volume 115(102825). <https://doi.org/10.1016/j.pce.2019.102825>.
- Zhou, L. M., Dickinson, R. E., Tian, Y. H., Fang, J. Y., Li, Q. X., Kaufman, R. K., Tucker, C. J. & Myneni, R. B. (2004). Evidence for a significant urbanization effect on climate in China. *Proceedings of the National Academy of Sciences of the United States of America*. Volume 101, pp 9540–9544.

Pratheep Kumar B.*

Assistant Professor,
Department of geography,
Government Arts and Science College
Kulathoor, Kerala University,
Thiruvananthapuram, Kerala

Emayavaramban V.

Professor and Head,
Department of Geography,
Madurai Kamaraj University,
Madurai, Tamilnadu

Author for Correspondence*

E-mail: pratheepgeo@gmail.com

